한국기계가공학회지, 제19권, 제12호, pp. 14~20(2020.12) ISSN 1598-6721(Print)
Journal of the Korean Society of Manufacturing Process Engineers, Vol. 19, No. 12, pp. 14~20(2020.12)ISSN 2288-0771(Online)

https://doi.org/10.14775/ksmpe.2020.19.12.014

A Study on the Optimal Design for Lightweight Vehicle Dash

Gyung-Il Lee*,#

*Department of Undeclared Majors, Songwon University

차량 Dash 경량화를 위한 최적설계에 관한 연구

이경일*,#

*송원대학교 자율전공학과

(Received 28 September 2020; received in revised form 05 October 2020; accepted 11 October 2020)

ABSTRACT

Currently, the automotive market is intensively researching eco-friendly vehicles such as EV vehicles and hydrogen vehicles. Further, research and developments for the future markets such as autonomous vehicles and the connective cars are coped up continuously along with the rising fuel economy regulations and the emission regulations. In this development, various sensors, batteries, and control devices are fused in order to decrease the weight of the vehicle. Moreover, since the fuel economy regulation is an issue, research on the weight reduction of body parts is underway. Therefore, in this work, a study is conducted to obtain the optimal design of the Dash part that separates the engine room and the passenger seat of the vehicle body by combining lightweight materials with high rigidity materials. The optimal design was obtained using the Finite Element Analysis. Further, AL5083 was used as the lightweight material and ASBC1470 was used for high strength materials. The parts made with this combination of materials had strength equivalent to that of the existing steel and the weight was reduced by 10%.

Key Words : Lightweight(경량화), Optimal Design(최적설계), Multi-Material Bonding(이종소재접합), Finite Element Analysis(유한요소해석)

1. Introduction

Regulations on higher fuel economy and reduced exhaust gas emissions have currently been tightened in the automobile market. Therefore, research and development for future markets, such as autonomous and connected vehicles, and intensive research on eco-friendly vehicles, such as electronic vehicles (EVs) and hydrogen vehicles, are in progress. However, this development has inevitably resulted in increasing the vehicle towing weight to the fusion of various sensors, batteries, and control devices. Hence, most studies have focused on reducing the weight of vehicle body parts[1].

There are various lightweight automobile technologies such as structural optimization and new process technology. Structural optimization is a method of reducing weight by optimizing the vehicle body structure, such as changing the shape or layout of

Corresponding Author : jia789@songwon.ac.kr
Tel: +82-62-360-5729, Fax: +82-62-360-5729

vehicle body components. In contrast, a new process technology attempts to reduce weight using other lightweight and high-strength materials than the existing ones. Therefore, this study investigates the optimal design by applying a combination of lightweight and high-stiffness materials to the dashboard parts separating the engine room and the boarding seat of the vehicle body, which were previously manufactured through a combination of lightweight and high-strength materials. The optimal design was achieved through the finite element method (FEM). Moreover, AL5083 and ASBC1470 were used as lightweight and high-strength materials to obtain equivalent stiffness compared to conventional steel, resulting in weight reduction by 24%[1,2].

2. Lightweight Dash Panel Design

2.1 Lightweight Design: 3D Modelling

The dash panel was designed to achieve the equivalent stiffness and 10% weight reduction compared to the conventional vehicle body. As shown in Fig. 1, AL5083 was utilized in designing lightweight material, and ASBC1470 was used to design reinforcement to overcome insufficient strength. ASBC1470 was selected as 1.4t, and AL5083 was 3D modeled at a level of approximately 1.2t-2.3t, owing to their press forming process and formability characteristics.

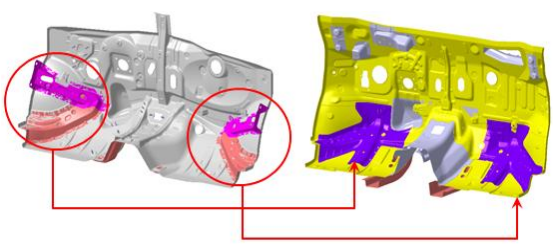

Fig. 1 Dash 3D modelling and comparison of reinforcement

(a) Dash Lwr Upr

(b) Dash Lwr Lh/Rh

Fig. 2 Dash Upr/Lwr 3D modelling

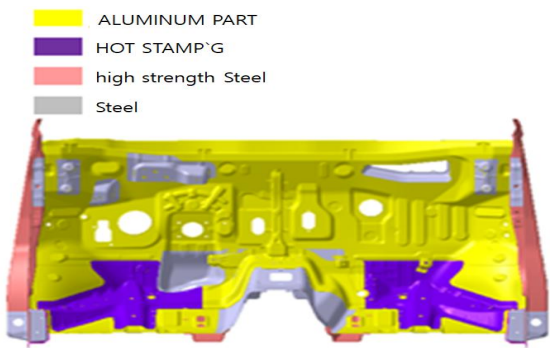

Fig. 3 Dash multi-material 3D modelling

Additionally, the dash cross side structure of the conventional mass-produced vehicles was divided into Upr/Lwr; Lwr was further divided into Lh and Rh to secure formability. Fig. 2(a) shows dash Upr; Fig. 2(b) shows dash Lwr Lh and Lwr Rh. Moreover, the application of multi-materials to dash is shown in Fig. 3

3. Optimal Dash Panel Design

3.1 FEM

Each element has a node corresponding to the vertex of the brick. The node becomes the point where each element joins. Therefore, a node is shared by two or more elements. Here, the word “join” refers to a complete attachment. According to

the mechanical theory, when an element is deformed due to an external force, the neighboring elements are also deformed. Hence, the deformation of the entire object can be calculated by measuring the deformation of each element. The increasing number of elements naturally requires more calculation. The basic calculation method remains the same irrespective of the shape of the object because the FEM divides an object into many elements and performs the calculation on each element.

3.2 Load-Stress Equilibrium Equation

Assume that V is a volume and S is a surface area of a certain 3D object. Any point within the object is represented by x,y, and z coordinates. Some parts of the object boundary, where displacement is applied, are constrained, as shown in Fig. . There is an exerting surface force vector (traction) T in other parts of the boundary, representing the distributed force per unit area. When a force is applied, an object deforms. The deformation at a point x $(=[x,y,z]^T)$is expressed by three components of the displacement, as shown in Equation (1) [3,4].

$$\mathrm{u} = [u,v,w]^T \tag{1}$$

Equation (2) expresses the distributed force per unit volume equal to the weight per unit volume as a vector, f.[3,4].

$$\mathrm{f} = [f_x,f_y,f_z]^T \tag{2}$$

Fig. 4 shows body force acting on a small cube of volume dV. The surface force vector, T, can be expressed as a vector component at any point on the surface. Examples of the stress vector include the distribution of contact force and the action of pressure. The load, P acting on a point I is represented by three components [3,4,5].

$$P_i = [P_x,P_y,P_z]_i^T \tag{3}$$

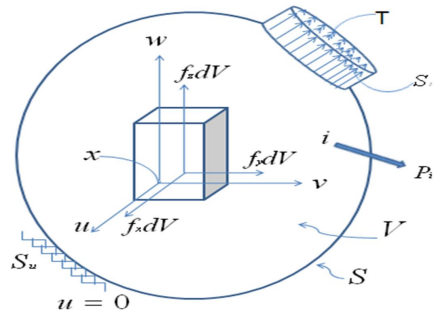

Fig. 4 3-D geometry

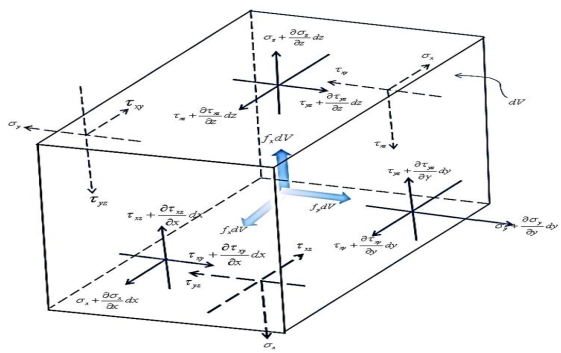

Fig. 5 The equilibrium of tiny volume

Fig. 5 shows the stress acting on a small cube of volume dV. When the volume is reduced to one point, the stress tensor can be expressed by arranging the components in a (3 X 3) symmetric matrix. However, as shown in Equation (4), the stress can be represented by six unique components.

$$\sigma = [\sigma_x,\sigma_y,\sigma_z,\tau_{yz},\tau_{xz},\tau_{xy}]^T \tag{4}$$

where $\sigma_x,\sigma_y,\sigma_z$ refer to the normal stress and $\tau_{yz},\tau_{xz},\tau_{xyz}$ denote the shear stress. Consider the volume equilibrium shown in Fig. 5. First, the force acting on the surface is obtained by multiplying the stress-applied area by the stress.

If $\sum F_x = 0, \sum F_y = 0, \sum F_z = 0$ and $dV = dxdydz$ the equilibrium equation is derived, as shown in Equation (5)[7,8,9].

$$\begin{aligned} \frac{\partial \sigma_x}{\partial x} + \frac{\partial \tau_{xy}}{\partial y} + \frac{\partial \tau_{xz}}{\partial z} + \int_x = 0 \\ \frac{\partial \tau_{xy}}{\partial x} + \frac{\partial \sigma_y}{\partial y} + \frac{\partial \tau_{yz}}{\partial z} + \int_y = 0 \\ \frac{\partial \tau_{xy}}{\partial x} + \frac{\partial \tau_{yz}}{\partial y} + \frac{\partial \sigma_z}{\partial z} + \int_z = 0 \end{aligned} \quad (5)$$

The boundary conditions include displacement conditions and surface load conditions, as shown in Fig. 6. If u is given at the boundary represented by S_u it is equivalent to Equation (6).[3,4]

$$S_u \text{ on } u = 0 \quad (6)$$

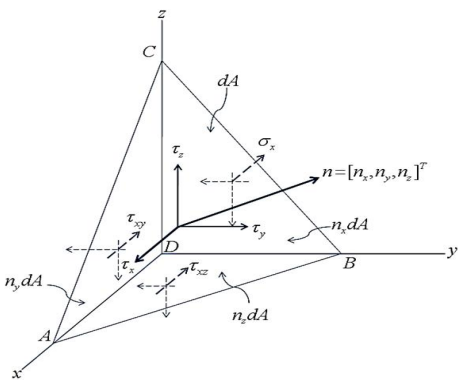

Fig. 6 The neighbors on the surface of tiny volume

Additionally, if the displacement is given by $a$the boundary condition can be represented as $u = a$. The equilibrium of the tetrahedral volume $ABCD$ is shown in Fig. 6. DA, DB, DC is parallel to each axis, x, y, z and the area ABC, represented by dA, is located on the surface. If $n = [n_x, n_y, n_z]^T$ is a unit vector perpendicular to dAt hen it corresponds to areas $BDC = n_x dA$, $ADC = n_y dA$, and $ADB = n_z dA$, respectively.

3.3 Optimal Design through Dash FEM

The degree of strength was measured to analyze the dash using the combined specimen of AL5083 and ASBC1470. A multi-lamination was performed using a joining agent and a rivet. The joining strength of the specimen was measured to be 12.51KN, as shown in Fig. 7.

The dash analysis implements the stiffness as in the conventional vehicle body and calculates the thickness of the AL5083 material to derive weight reduction. Moreover, the airbag—a safety device in the event of a frontal collision—acts as a collision detecting sensor. However, the optimal design was implemented by allowing hot spot stress and deformation to occur in one section of the dash if the airbag fails to operate owing to the sensor malfunctioning during a sudden stop in the event of a collision. Dash was designed to mechanically operate the airbag through hot spot deformation. Fig. 8 shows the result of the dash analysis. ANSYS—a commercial FEM tool— was utilized for the analysis. We equally applied a 13.85 kN load

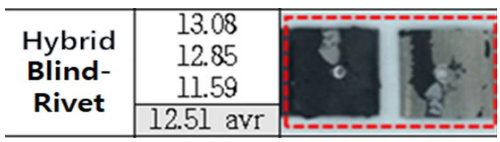

Fig. 7 Dash hybrid bonding strength

Table 1 Deformation amount by thickness

	Deformation
Existing product	0.001211
Material change 1.2t	0.002088
Material change 1.5t	0.001484
Material change 2t	0.001063
Material change 2.3t	0.000911

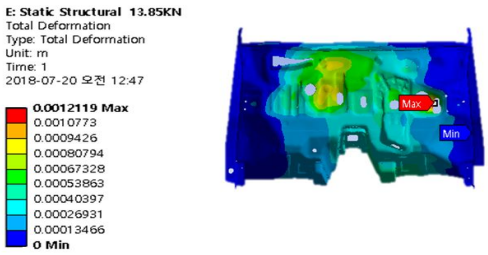

(a) Existing product deformation

(b) Existing product stress

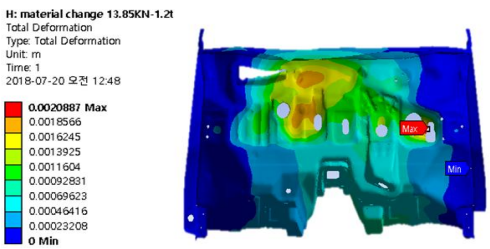

(c) AL5083(1.2t) deformation

(d) AL5083(1.2t) stress

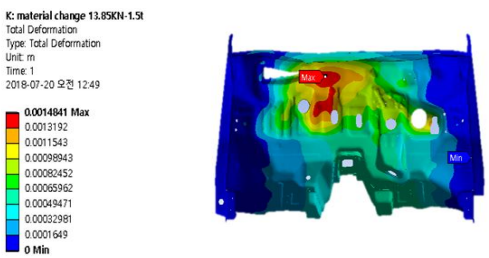

(e) AL5083(1.5t) deformation

(f) AL5083(1.5t) stress

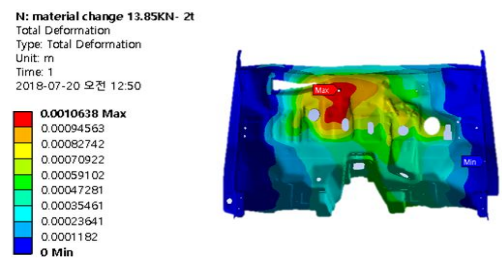

(g)AL5083(2t) deformation

(h) AL5083(2t) stress

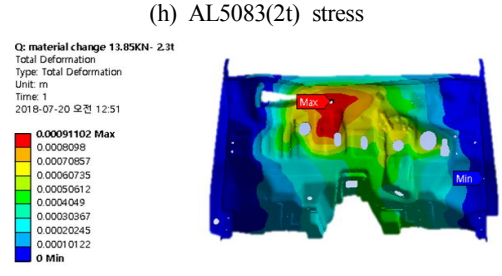

(i)AL5083(2.3t) deformation

(j) AL5083(2.3t) stress

Fig. 8 Dash FEM finite element analysis results

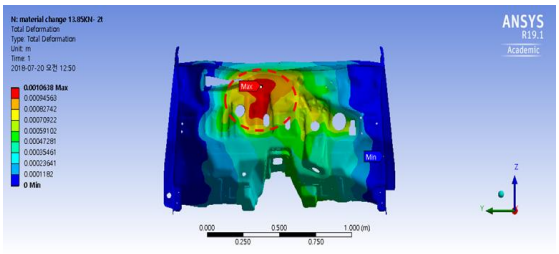

Fig. 9 Dash deformation focus

Table 2 Dash weight comparison table

Part Name	Design weight (g)		Actual weight (g)	Weight difference (g)	ratio (%)
	Existing body	Lightweight body			
Dash Upr	6,580	3,776	3,762	2,804	43%
Dash Lwr, Lh	2,280	1,741	1,732	539	24%
Dash Lwr, Rh	2,309	1,763	1,735	546	24%

Fig. 10 Lightweight Dash actual weight

As shown in Table 1, The dash analysis result shows that the AL5082 material has the same stiffness as found in the conventional vehicle body when it is 2t or higher; deformation is concentrated as shown in Fig. 9.

4. Dash Weight Reduction

The weight reduction was confirmed by comparing the designed weights of the conventional vehicle body with the designed and actual weights of the lightweight vehicle body. Table 2 shows the material, thickness, and weight of the conventional and lightweight vehicle bodies. Fig. 10 illustrates the weight of the lightweight vehicle body.

5. Results and Discussion

This study implements equivalent stiffness using multi-materials for dash parts of the vehicle body to improve fuel economy in accordance with fuel economy regulations for vehicles. We managed to achieve a 24% lighter vehicle body weight.

1. The thickness of AL5083 was more than equal to 2t, which was used to reduce the weight of the dash. Moreover, the analysis shows that it is possible to achieve the same stiffness as in the conventional vehicle body by joining ASBC1470 with adhesive and rivet.
2. Through the design using ASBC1470, and when the thickness of Dash's AL5083 material is applied with 2t or more, and it is possible to achieve 24% weight reduction compared to the conventional vehicle body using ASBC1470 in designing and AL5082 with more than equal to 2t thickness in the dash. This weight reduction is higher than the target of 10%.

Acknowledgments

This study was conducted with support from Songwon University's academic research funding in 2020 (Project No.: A2020-43)

REFERENCES

1. Jung, Y. S., Lee, G. I., Kim, J. Y., "Study on Optimal Design of F-Apron of Vehicles by Multi-material Bonding," Journal of the Korean Society of Manufacturing Process Engineers, Vol. 18, No. 02, pp. 102-107, 2019.
2. Gao, J. C., Kim, J. Y., "Simulation for Improvement of Temperature Distribution Inside Refrigerator," Journal of the Korean Society of Manufacturing Process Engineers,, Vol. 18, No.

12, pp. 98-103, 2019.
3. Ahn, T. K., Lee, Y. J., Lee, S. C., "A Study on Composite Materials Frame of Electric Vehicles using Collision Analysis," Journal of the Korean Society of Manufacturing Process Engineers, Vol. 19, No. 02, pp. 75-80, 2020.
4. Kim, C. W., Yoo, J. I., Choi, S. D., Hur, J. W., "An Evaluation of Pneumatic Conveyor Equipment Stability Through Fluid Structure Interface Analysis," Journal of the Korean Society of Manufacturing Process Engineers, Vol. 18, No. 09, pp. 94-99, 2019.
5. Lee, G. L., and Kim, J. Y., Gao, J. C., Jung, Y. S., “Study of Heat Generation and Cutting Accuracy depending on Spindle Rotation Speed Change in Ultra-precision Cutting Using ECTS,” IJPEM, pp. 265-269, 2018.
6. Sim, K. J., Moon, H. J., Jeon, N. J., “A Study on the Development of the Driveshaft for a 3.5-Ton Commercial Vehicle,” Journal of the Korean Society of Manufacturing Process Engineers, Vol. 17, No. 2, pp. 153-159, 2018.
7. Geyl, R., "Design and Farication of Three-Mirror Flat-Field Anastigmat for High-Resolution Earth Observation," SPIE, Vol.2210, pp.739-745, 1994.
8. Patterson, S. R., Matgab, E. B., "Design and Testing of a Fast Tool Servo for Diamond Turing," Precision Engineering, Vol. 7, No.3, pp.123-128, 1985.